Designing stability into thermally reactive plumbylenes

Goran Bačić,[*,†,¶] David Zanders,[‡,¶] Anjana Devi,[‡] and Seán T. Barry[†]

†*Department of Chemistry, Carleton University, 1125 Colonel By Drive, Ottawa, Ontario, Canada K1S 5B6*

‡*Inorganic Materials Chemistry, Ruhr-Universität Bochum, 44801 Bochum, Germany*

¶*Contributed equally to this work*

E-mail: gibacic@gmail.com

Abstract

Lead analogues of *N*-heterocyclic carbenes (NHPbs) are the least understood members of this increasingly important class of compounds. Here we report the design, preparation, isolation, structure, volatility and decomposition pathways of a novel aliphatic NHPb: *rac*-N^2,N^3-di-*tert*-butylbutane-2,3-diamido lead(II) (**1Pb**). High steric hindrance of the *tert*-butylamido moeities and *rac*-butane backbone successfully block redox decomposition pathways observed for diamidoethylene and -ethane backbone analogues, pushing the onset of thermal decomposition above 150 °C. With a high vapour pressure of 1 Torr at 94±2 °C and exceptional thermal stability among Pb(II) complexes, **1Pb** is a promising precursor for the chemical vapour deposition (CVD) and atomic layer deposition (ALD) of functional lead-containing materials.

Introduction

Lead-containing materials like ferroelectric Pb(Zr,Ti)O_3 (PZT) and organolead halide perovskites (e.g. $CH_3NH_3PbI_3$) are high-performance and increasingly important functional materials for next-generation memory[1] and solar cells,[2] and lead (II) chalcogenide (e.g. PbS) nanocrystals have been shown to possess promising quantum mechanical properties such as band-gap tuning by quantum confinement[3,4] and quantum efficiencies over unity by multiexciton generation (MEG).[5,6] Future device architectures will require subnanometer thickness control, emphasizing the need for accessible lead-containing precursors for fabrication techniques like chemical vapour deposition (CVD) and atomic layer deposition (ALD). However, known precursors are scarce, and available chemical precursors are either too hazardous (e.g. Et_4Pb) or non-volatile (e.g Pb(II) β-diketonates)[7] to be practical in either an industry or research setting. For example, the most common lead-containing vapour phase precursor, lead (II) bis(2,2,6,6-tetramethyl-3,5-heptanedionate) [Pb(tmhd)$_2$], has a very low vapour pressure of 0.05 Torr at a realtively high temperature of 180 °C,[8] rendering it impractical for use in commercial reactors that typically operate at 1 Torr. This issue is exacerbated by a small available library of volatile Pb complexes to choose as potential chemical precursors, and manifests in relatively rare examples of ALD of lead-containing materials.[9]

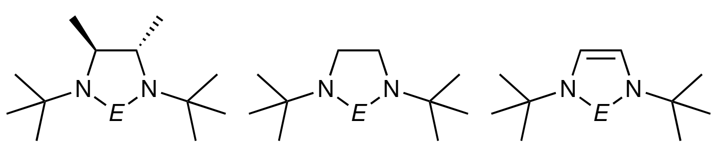

Scheme 1: General scheme and nomenclature for divalent *N*-heterocyclic metallylenes (NH*E*s). Backbone functionalization is denoted as follows: dimethylated (**1*E***), hydrogenated (**2*E***), and unsaturated (**3*E***) where *E* = Si-Pb.

N-heterocyclic metallylenes (NH*E*s, where *E* = Si-Pb, Scheme 1) are an emerging class of compounds that are competent and versatile ligands for homogeneous catalysis,[10–12] as well as volatile, thermally stable and chemically reactive precursors for CVD[13] and ALD.[14] Although **2Ge**,[13] **1Ge** and **1Sn**[14] have seen significant employment as vapour-phase precursor compounds, the corresponding lead analogues (NHPbs) have not received the same attention. The number of examples of these compounds decreases when descending the group, and to date there is only one failed preparation of the **3Pb** analogue.[15] Previously reported saturated NHPbs are often dimeric, and stabilized by sterically hindering the Pb(II) center at the nitrogen chelate positions with bulky, electron-rich aryl[16] or $SiMe_3$[17] groups. Even monomeric benzannulated and aryl-amino functionalized NHPbs display significant intermolecular interaction via π-π stacking.[16,18] Dimerization can impart significant disadvantages on the volatility of discrete molecular compounds due to the Knudsen relationship between vapour pressure and molecular weight, and is best avoided in the design of precursors for heavy metals like Pb.[19] Additionally, even monomeric aryl-functionalized NHPbs are likely too heavy to be practically volatile, and neither they nor their congeners have been reported to have been purified by sublimation or distillation.

We thus considered previously reported NHPb species unsuitable as potential precursors, and a different path was explored to prepare a monomeric, volatile and thermally robust NHPb for ALD. We were motivated to explore the thermal chemistry of a relatively unknown family of aliphatic NHPb analogues due to their low molecular weight, resistance to dimerization,[20] as well as the overall lack of practical precursors for ALD of lead-containing materials. Here, we report the attempted syntheses and decomposition pathways of two NHPb derivatives **2Pb** and **3Pb**, and the successful preparation, structural analysis, thermal characterization and decomposition pathway of *rac*-N^2,N^3-di-*tert*-butylbutane-2,3-diamido lead(II) (**1Pb**).

Results and Discussion

N^2,N^3-di-*tert*-butylethylene-2,3-diamido lead(II) (3Pb)

We first sought to reproduce literature reports and attempt to synthesize the 6π-aromatic **3Pb** by salt-metathesis with N, N'-di-*tert*-butyl-N, N'-dilithiodiazadienide, and transamination with N, N'-di-*tert*-butyl-1-aldimino-2-amine (aldimine).[15] Both pathways resulted in the precipitation of black Pb(0) particles and the parent N, N'-di-*tert*-butylethylene-1,2-diimine at −78 °C (Scheme 2), which could be recovered in high yield (>90%) by sublimation from the residue after removal of solvent.

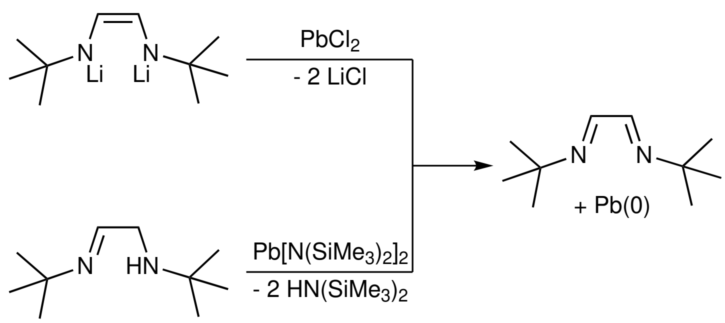

Scheme 2: [4+1] cycloreversion upon attempted syntheses of **3Pb** by salt metathesis with dilithiated diazadienide or transamination with *N*, *N′*-di-*tert*-butyl-1-aldimino-2-amine. The resulting diimine can be recovered in high yield by sublimation directly from the residue.

Isolation of the target **3Pb** was not attempted as decomposition occured far below room temperature, and the intermediate from the transamination is reported to decompose before forming the heterocycle.[15]

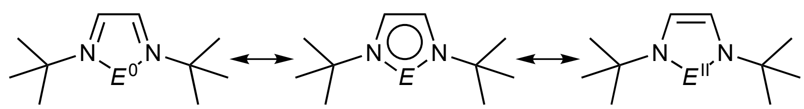

Scheme 3: Unsaturated NH*E*s are 6π-aromatic rings. Historically, and for the lighter congeners, the ylene character (right) is emphasized over the ylone (left). The zero-valent description becomes increasingly important when descending the group.

This marked instability is in stark contrast to the exceptional stability of **3Si** and **3Ge**, which thermolyze at 220 and 626 °C, respectively.[13,21] However, **3Sn** is reported to decompose at a mild 60 °C,[15] supporting an increasingly non-innocent character of the diimine ligand when descending the group. Historically, the formally zero-valent (i.e. ylone, chelated atom) description of **3*E*** was considered an exaggeration of the aromatic resonance,[22] and the compounds are typically depicted as divalent ylenes. Recently, attempts to form **3*E***$\rightarrow$AeCp$^*_2$ coordination complexes of the alkaline earth metals (Ae = Ca-Ba) with **3Si** and **3Ge** produced the *N*, *N′*-di-*tert*-butylethylene-1,2-diimine adducts AeCp$^*_2$(DAD) and crystalline Si(0) and Ge(0), respectively, even during recrystallization at −40 °C.[23] This unusual formal reduction of Si and Ge was rationalized as being due to a significant zero-valent character being expressed by **3*E*** compounds, which allows for transfer of the diimine from a naked *E*(0) to AeCp$^*_2$. Similar naked atom transfers were reported for **3Sn** with other diimines,[15] and for **3Pb** the solely ylone character prevents its isolation.

N^2,*N*^{3}-di-*tert*-butylethane-2,3-diamido lead(II) (2Pb)

We then attempted to prepare the saturated **2Pb** by transamination of $Pb[N(SiMe_3)_2]_2$ with free N,N'-di-*tert*-butylethylene-1,2-diamine in toluene. Turbidity developed immediately upon addition of diamine and within minutes a dark precipitate had formed. After the mixture was stirred for two days in the dark, ^{1}H and ^{13}C NMR revealed no starting $Pb[N(SiMe_3)_2]_2$ remained and signals for N,N'-di-*tert*-butylethylene-1,2-diimine were observed. We suspect the bimolecular formal dehydrogenation reported for **2Ge**[13,24] occurs readily with lead, so we performed in-situ ^{1}H NMR to gain insight to the decomposition pathway, as shown in Scheme 4 and Figure 1.

Starting reactants were consumed rapidly and were undetectable the next day, while signals very similar to the *tert*-butyl groups [δ = 1.35 ppm (br, 9H) and δ = 1.03 ppm (br, 9H)] of the 3-coordinate intermediate **5Pb**[15] appeared within a few minutes and increased over the duration of the experiment. It is likely the chemical shifts of the analogous groups on **4Pb** are indistinguishable from the oxidized **5Pb** considering the peak-broadening from poor shimming due to precipitation of Pb(0) as the reaction proceeded. We believe **4Pb** to be the main reaction intermediate, as its redox decomposition releases diamine to react with further $Pb[N(SiMe_3)_2]_2$ and replenish its concentration, and the $-N(SiMe_3)_2$ signal for **4Pb/5Pb** remained constant. The signals corresponding to N=C*H* (δ = 8.08 ppm) imino and *tert*-butyl protons (δ = 1.17 ppm) N,N'-di-*tert*-butylethylene-1,2-diimine increased monotonically, and after 5 days free $HN(SiMe_3)_2$, diamine and diimine were the only detectable species by ^{1}H, ^{13}C, HSQC and COSY NMR spectroscopy, confirmed with respect to authentic samples.

Decomposition begins when the diamine exchanges with one $-N(SiMe_3)_2$ group on $Pb[N(SiMe_3)_2]_2$ to form **4Pb**, which then eliminates Pb(0), free diamine, $HN(SiMe_3)_2$ and **5Pb** by oxidation of the Pb-amido group to an imine and deprotonation of the unchelated amine to form a chelated amido group. **5Pb** then undergoes a second bimolecular deprotonation to form $HN(SiMe_3)_2$ and **3Pb** followed by [4+1] cycloreversion to diimine and Pb(0). Similar backbone deprotonation by

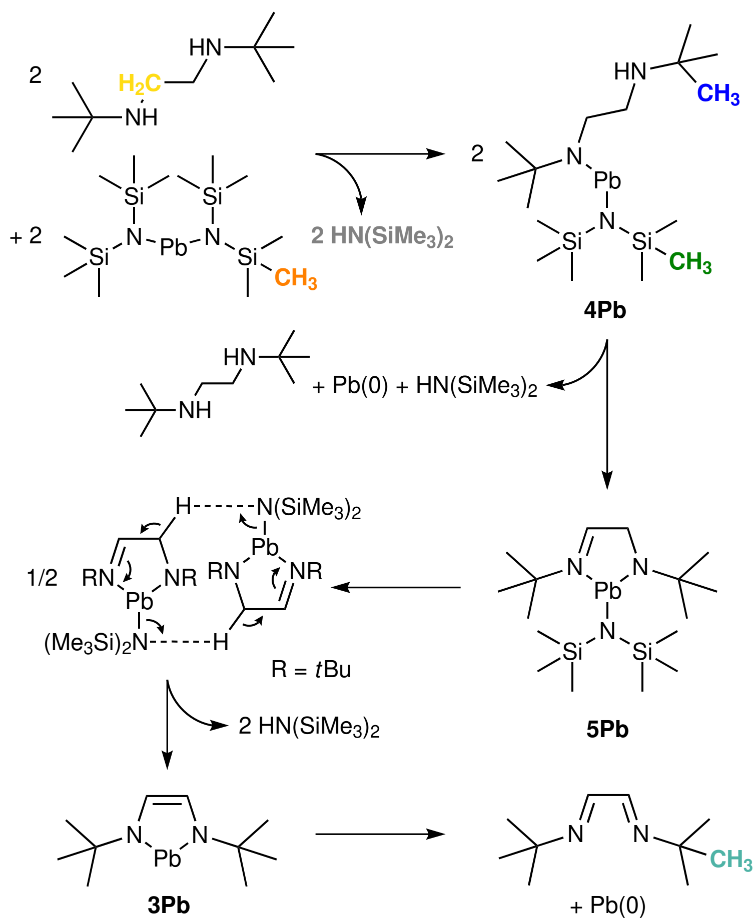

Scheme 4: Attempted preparation of **2Pb** by transamination at room temperature results in bimolecular decomposition by formal dehydrogenation of *N*, *N′*-di-*tert*-butylethylene-1,2-diamine to *N*, *N′*-di-*tert*-butylethylene-1,2-diimine. In-situ ^{1}H NMR suggests the formation of the intermediate **4Pb** which undergoes bimolecular redox to release free diamine, $HN(SiMe_3)_2$ and Pb(0), and generate the amido-α-aldimine intermediate **5Pb**. This subsequently undergoes another bimolecular deprotonation to form **3Pb** which then decomposes to diimine and Pb(0) by [4+1] cycloreversion via the formally zero-valent diimino plumbylone. The colour of bolded moieties correspond to the protons tracked during in-situ ^{1}H NMR spectroscopy of this reaction, shown in Figure 1.

$HN(SiMe_3)_2$ of an NHC was observed previously in our group with Cu(I) NHC complexes.[25] Diamine and diimine are found in a 2:3 ratio upon completion of the reaction, implying the exchange of $-N(SiMe_3)_2$ moeities on **4Pb** or **5Pb** during reaction with diamine, which convert more diamine to diimine upon decomposition.

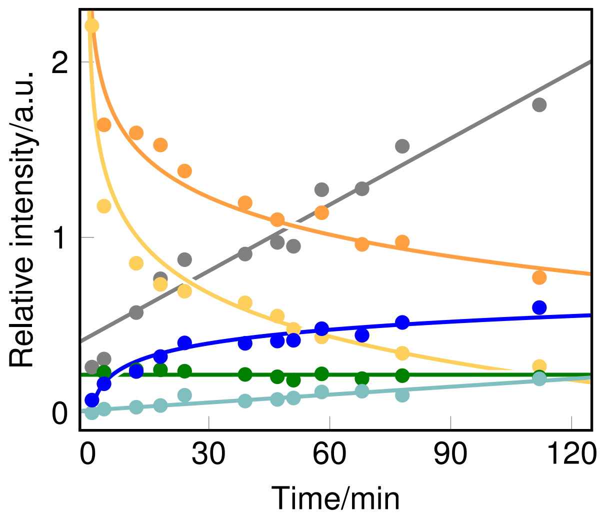

Figure 1: In-situ ^1H NMR of the first two hours of the attempted synthesis of **2Pb** reveals decomposition via the intermediate **4Pb**, which subsequently undergoes formal dehydrogenation to **5Pb**, the previously observed in the attempted synthesis of **3Pb** via aldimine transamination.[15] Relative intensity is the integration of a respective peak calibrated with respect to residual C_6H_6, divided by the number of those protons per species (e.g. by a factor of 18 for $HN(SiMe_3)_2$). Lines and curves are aids to the eye. $Pb[N(SiMe_3)_2]_2$ (orange ●) and *rac*-*N*, *N′*-di-*tert*-butylbutane-1,2-diamine (yellow ●) are consumed rapidly, while $HN(SiMe_3)_2$ (gray ●) is produced steadily. Signals for *tert*-butyl (blue ●) and $-N(SiMe_3)_2$ (green ●) protons on **4Pb** suggest it quickly forms an equilibrium as the main reaction intermediate. Clear signals for *tert*-butyl groups on *N*, *N′*-di-*tert*-butylethylene-1,2-diimine (teal ●) grow steadily, finally resulting in a diamine:diimine ratio of 2:3 after 5 days.

Rac-*N*,[2]*N*[3]-di-*tert*-butylbutane-2,3-diamido lead(II)(1Pb)

Failure to isolate **2Pb** or **3Pb** prompted us to design a plumbylene in which oxidation of the amido group of the 3-coordinate intermediate is blocked by increased steric bulk at the backbone carbon bridge, and so the title-compound *rac*-*N*,[2]*N*[3]-di-*tert*-butylbutane-2,3-diamido lead(II) (**1Pb**) was prepared. Salt-metathesis of $PbCl_2$ with dilithiated butanediamido salt in diethyl ether produced a black crystalline precipitate upon warming from −78 °C to room temperature, which we determined by workup to contain very small amounts **1Pb** (NMR), Pb(0) (insoluble in water, 6N HCl; soluble in 6N HNO_3), LiCl (dissolved in water leaving behind black Pb(0)), and an imine (NMR). Presumably, $PbCl_2$ oxidizes the diamido salt to produce a similar product as upon thermolysis, later identified as acetaldehyde *tert*-butylimine (Scheme 6).

The yield of intended product was improved to 85% by transamination of $Pb[N(SiMe_3)_2]_2$ with one equivalent of the free diamine ligand in hexanes or toluene (Scheme 5), which is a synthetic route that has been previously reported to access other NHPbs.[16,18] The transamination required considerable heating and time (70 °C, 3 days) to proceed completely, likely due to the high steric demand of the desired diamine and the leaving $–N(SiMe_3)_2$ ligands. Removal of solvent by vacuum results in a red oil that is a mixture of **1Pb** and free diamine, which cannot be separated by simple distillation. Pure **1Pb** is isolated from the oil as blood-red needle-like crystals (m.p. 53 °C) by fractional sublimation under dynamic vacuum onto a water-cooled finger. Briefly, free diamine was slowly removed and collected in a liquid-nitrogen cold trap, while any impure oil that collected on the water-cooled cold finger refluxed until only **1Pb** remained, which then sublimed at 45-55 °C/50 mTorr.

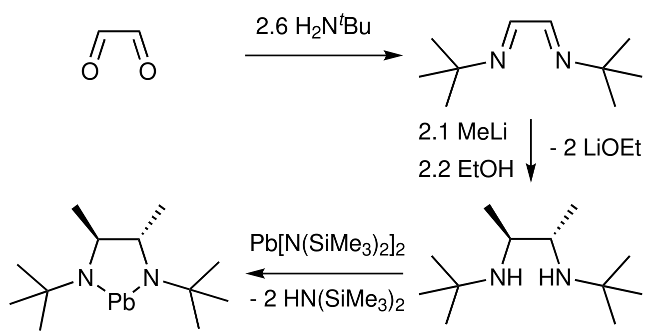

Scheme 5: Synthesis of **1Pb** by transamination. (a) Glyoxal is converted to di-*tert*-butyl-diazabutadiene (DAD) with $^{t}BuNH_2$ in Et_2O, (b) then methylated by 2eq. MeLi in Et_2O and protonated by an excess of EtOH. (c) Transamination with $Pb[N(SiMe_3)_2]_2$ at 70°C for 3 days yields the title compound in high yield.

Notably, unlike acyclic diamido Pb(II) complexes, **1Pb** is not noticebly thermochromic, and maintains its colour during distillation and upon cooling in a −40 °C freezer. In contrast, $Pb[N(SiMe_3)_2]_2$ becomes ruby red during distillation, cools to an orange solid at room-temperature, is yellow in the same −40 °C freezer, and becomes colourless in liquid nitrogen. We hypothesize that the lack of thermochromicity this may be due to the limited range of N–Pb–N angles available to cyclic diamido plumbylenes like **1Pb** (79.9° in the solid-state at 140 K, Figure 2), whereas the acyclic $Pb[N(SiMe_3)_2]_2$ is reported to change its bond angle dramatically: from 91° in the gas-phase to 103.2° in the solid-state at 140 K.[26]

Solid-state and solution-phase structure

We performed solid-state single crystal X-ray diffraction (scXRD) crystallography on **1Pb** to determine its structure and degree of intermolecular interaction. The ligand is synthesized as a 1:1 racemic mixture that is not separated during purification, and the resulting **1Pb** complex is also obtained as a 1:1 racemic mixture. Both enantiomers are present in its asymmetric unit cell (Figure 2). Torsion of the backbone carbons and *tert*-butyl moieties suggests their intramolecular repulsion is due to the significant steric bulk of the ligand.

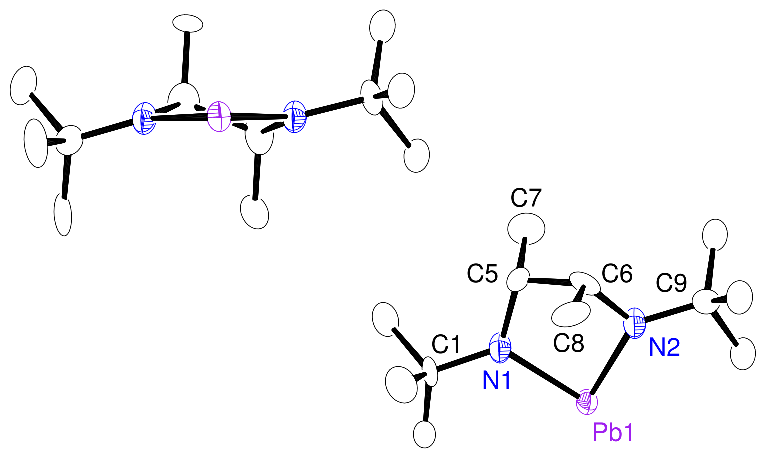

Figure 2: Asymmetric unit of **1Pb** in the solid-state showing both *S,S* (left) and *R,R* (right) enantiomers. Ellipsoids set at 50% probability. Hydrogen atoms omitted for clarity. Selected bond lengths (Å) and angles (°): Pb(1)−N(1) = 2.16 (1), Pb(1)−N(2) = 2.12 (1); N(1)−Pb(1)−N(2) = 79.9 (6), Pb(1)−N(1)−C(5) = 113 (1), Pb(1)−N(2)−C(6) = 111 (1), Pb(1)−N(1)−C(1) = 126 (1), Pb(1)−N(2)−C(9) = 130 (1).

Intermolecular interactions that are seen with less sterically demanding ligands[17] were successfully hindered by the steric bulk of the *tert*-butylamido functional groups and the racemic butane backbone, preventing dimerization. The stereochemically active 6s lone-pair on Pb(II) can also be inferred from the molecular structure of **1Pb**, where only one –CH_3 moiety from each *tert*-butylamido group faces the Pb center to reduce steric congestion. Alternating, enantiomerically selective (i.e. *S,S* or *R,R*) herringbone double-columns of **1Pb** are in the crystal structure (Figure 3), with the shortest Pb–Pb* distance being 4.127 Å. This repeating long-range interaction arises from electron density donation from the basic $6\,s^2$ lone-pair on one Pb(II) atom to the empty acidic $6p_z^0$ orbital on another in an opposite column. The NNPb–Pb* angle is 92.30°, which corresponds well with previously calculated $6s^2$ Lewis acid bonding for NN–Pb–M (M=Pt, Pd) complexes.[27] Additionally, the obtuse NN–Pb–Pb* angle suggests that there is no NN–Pb* π-interaction.

High-resolution ^{207}Pb NMR revealed a single peak (δ = +3488 ppm) that was only slightly more deshielded than the previously reported $N,^2N^3$-bis-2,6-di-*iso*-propylphenylethane-1,2-diamido lead(II) (δ = +3504 ppm),[16] suggesting **1Pb** is also monomeric in solution. NHPbs' intermolecular coordination in solution can be effectively probed by ^{207}Pb NMR: true dimers like $N,^2N^3$-bis-trimethylsilylethane-1,2-diamido lead(II)[17] are deshielded (δ = +403 ppm)[28] while NHPbs that are loosely associated dimers in solution show intermiediate shielding ($\delta \lesssim 3000$ ppm).[29] Monomeric Pb(II) diamides experience heavy shielding ($\delta = 3500-5000$ ppm),[28] however it remains difficult to explain the wide range of chemical shifts amongst monomeric species due to the dearth of reported spectra of NHPbs in the literature, and the unknown electronic effects of endo- and exocyclic silyl functionalization.

Volatility and thermal stability of 1Pb

We performed thermogravimetric analysis (TGA) of **1Pb** in Al_2O_3-passivated Pt pans to determine its volatility and thermal stability, and by extension its suitability as a vapour-phase precursor (Figure 4 and 5). Due to the kinetics of volatilization, higher initial mass loadings allow more mass of compound to be exposed to higher temperatures, allowing higher temperature decomposition to be probed during the experiment and the residual mass to increase.[30] Additionally, the derivative of

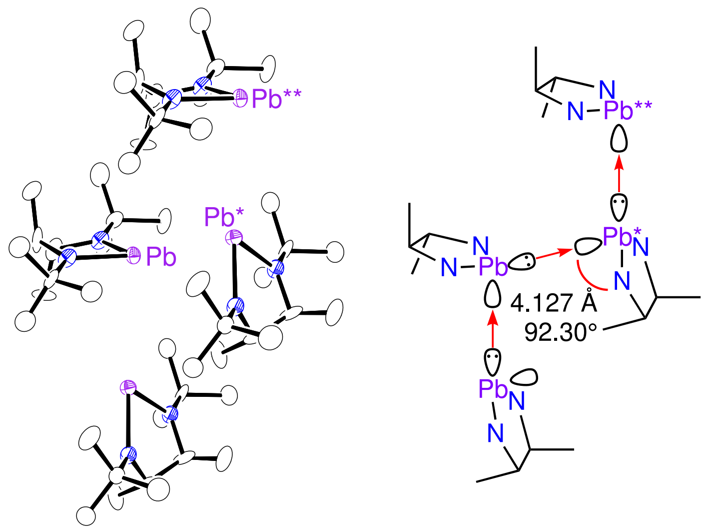

Figure 3: **1Pb** packs in alternating enantiomerically-selective herringbone double columns: shown here as *S,S* (side-on, left) with *R,R* columns (omitted) adjacent in the crystal structure. Long-range repeating Pb–Pb*–Pb** interactions (4.127 Å, 102.36°) presumably arise from repeating Lewis acid-base stabilization via $6\,s^2$ σ-donation to an empty $6p_z^0$ orbital (Pb–Pb*NN = 92.30°) in an opposite column, as depicted in the schematic (right, *tert*-butyl groups omitted for clarity).

mass with respect to temperature shows the onset of decomposition events as inflections. Together these methods provided useful estimates of the onset and extent of decomposition of **1Pb**. The higher mass loadings showed that decomposition began competing with volatilization around 160 °C, and residual mass increased from 1.2% to 4.0%. **1Pb** loses 1% of its initial mass at about 77 °C, and a small residual mass of 1.2% was left after being held at this temperature under flow-conditions. Under the same conditions, the well known $Pb[N(SiMe_3)_2]_2$ loses 1% of its initial mass at about 100 °C and leaves residual masses of 8.1% and 15.7% for 13 mg and 30 mg loadings. (See Supplementary Information for comparative TGA curves.)

The vapour pressure of **1Pb** was estimated by stepped isothermal TGA experiments,[31] and was found to volatilize according to Equation 1 (Figure 5).

$$\ln p = -5338.2T^{-1} + 15.914 \tag{1}$$

where p is the pressure in Torr, and T is the temperature in K. Accordingly, **1Pb** has a vapour pressure of 1 Torr at 94±2 °C, making it the most volatile Pb(II) compound reported, and among the most

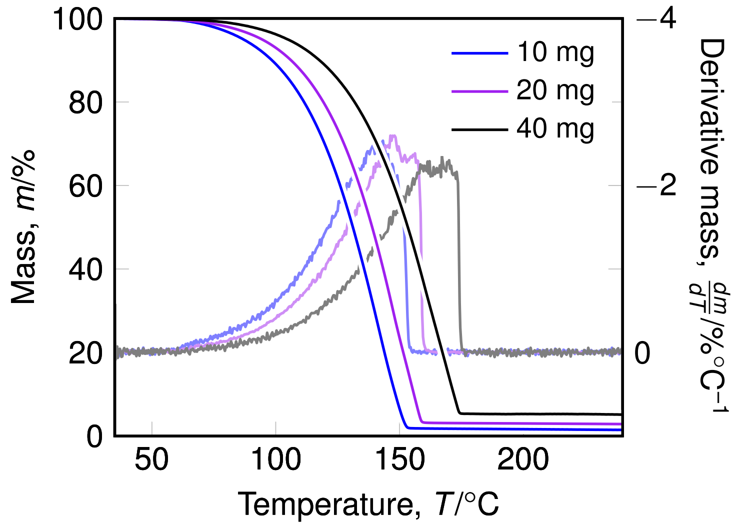

Figure 4: TGA of **1Pb** using 10 °C min^{-1} temperature ramp curves (front) and their derivatives (back) to assess thermal stability. The initial mass was increased from approximately 10 mg (blue), 20 mg (purple), to 40 mg (black) as a stress test on the compound, showing an increase in residual mass from 1.2%, 2.5%, to 4.0%, respectively. The emergence of secondary peaks in the derivative curves indicate the onset of decomposition at approximately 160 °C, which contributes to the increase in residual mass.

volatile Pb compounds known, behind only extremely hazardous tetraalkyl lead(IV) species like Et_4Pb.

Thermolysis products of 1Pb

Preliminary solution-phase decomposition studies by ^{1}H and ^{13}C NMR showed **1Pb** underwent some decomposition at 90 °C in toluene-d^8 with an estimated half-life of $t_{1/2}$ = 414 h. Thermolysis products were mostly free diamine ligand, and considering the lack of unsaturated diketimine, the analogous [4+1] cycloreversion did not occur.[13,23] It is likely trace protons were abstracted from the NMR tube's glass or through a small leak. Higher temperature decomposition in solution yielded spectra that were difficult to interpret, but the emergence of a shielded proton signal suggested the formation of an imine.

We heated a neat sample of **1Pb** under a stream of Ar below a reflux condenser and extracted the decomposed residue with benzene-d^6 to obtain better spectra with a higher concentration sample, and observed signals by ^{1}H, ^{13}C, COSY and HSQC NMR experiments that corresponded to

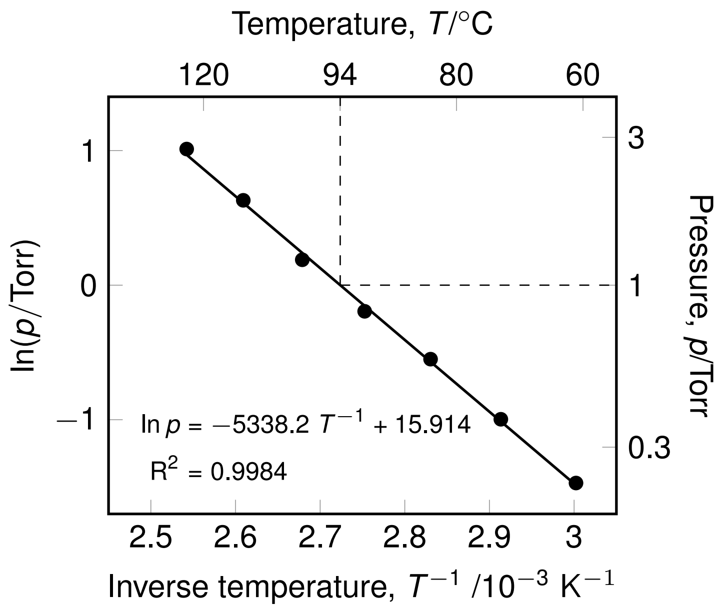

Figure 5: Vapour pressure of **1Pb** modelled according to the Langmuir equation as estimated by TGA under 1 atm N_2, displaying an extraordinary 1 Torr vapour pressure at 94±2 °C, as denoted by the dashed crosshairs. **1Pb** evaporates according to the equation $\ln p = -5338.2T^{-1} + 15.914$, where T is in K and p is in Torr.

acetaldehyde *tert*-butylimine [$\delta(^1H) = 7.62$ (q, 1H, CH=N) and $\delta = 1.71$ (d, 3H, =C(H)CH_3)],[32] suggesting that **1Pb** decomposes by reductive elimination of Pb(0) and oxidative cleavage of the backbone of the ligand as shown in Scheme 6. The increased steric demand of the *rac*-butane backbone of **1Pb** effectively protects it from following the same decomposition pathway observed for **2Pb**, pushing the thermal stability from below room temperature to above 150 °C, when the backbone cracks under unimolecular decomposition.

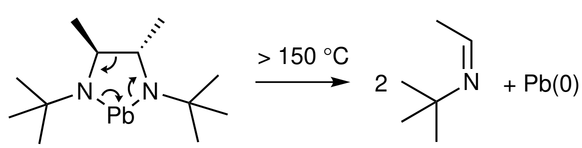

Scheme 6: [2+2+1] cycloreversion thermolysis of **1Pb** at 150 °C.

A mechanistic understanding of thermolysis is important for the development of robust ligand design and vapour deposition process, and the development of indefinitely robust precursors beyond **1Pb** would be attractive to industry for production settings, especially considering the successful development of **1Ge** and **1Sn**. Satisfying these conditions with novel diamido ligands is the subject of an ongoing investigation. Decomposition at vaporization temperatures (i.e. ca. 90 °C) is negligible, and its ease of synthesis makes it an attractive potential precursor.

Conclusion

Pb(II) was shown to oxidize N, N'-di-*tert*-butyl-N, N'-di-lithiodiamidoethylene and N, N'-di-*tert*-butyl-1-aldimino-2-amine, and also oxidize a fraction of N, N'-di-*tert*-butylethylene-1,2-diamine, cleanly to N, N'-di-*tert*-butylethylene-1,2-diimine. Steric hindrance of the C_2-bridge backbone with methyl groups blocks oxidation of the ligand and improves the stability of the heterocyclic ring system from below room temperature to above 150 °C. With exceptional volatility (94±2 °C) and thermal stability (ca. 150 °C), **1Pb** opens a window of over 60 °C between sufficient vapour pressure for delivery and the onset of thermal decomposition. It is a promising new CVD or ALD precursor for lead-containing materials, and stands in stark contrast to its ethane- and ethylene-backboned analogues.

Acknowledgements

The authors wish to thank Manuela Winter and Bert Mallick for supporting this work with crystallography, and Sharon Curtis and the University of Ottawa for mass spectrometry. S.T.B and G.B. acknowledge the QEII-OGSST Program and Carleton University for support. D.Z. thanks the PROMOS student exchange program (DAAD funded) for financial support.

Experimental Details

Synthesis

General Considerations

All manipulations were performed under air-free conditions using standard Schlenk techniques or in a N_2-filled (99.998% purity) MBraun Labmaster 130 dry-box unless otherwise specified. Glyoxal (40 wt.% in water), *tert*-butylamine (98%), MeLi (1.6 M in Et_2O), ^{n}BuLi (11.0 M in hexanes), hexamethyldisilazane [$HN(SiMe_3)_2$] (99%), and N, N'-di-*tert*-butylethane-2,3-diamine (98%) [$\delta_{^1\mathrm{H}}$ NMR (300 MHz, C_6D_6, $\delta_{C_6H_6}$ = 7.16 ppm): 1.05 (18H, *s*, $C(CH_3)_3$), 2.58 (4H, *q*, NCH_2), 0.7655 (4H, *q*, N*H*)). $\delta_{^{13}\mathrm{C}}$ NMR (300 MHz, C_6D_6, $\delta_{C_6\mathrm{H}_6}$ = 128.39 ppm): 29.72 ($C(CH_3)_3$), 43.9 (NCH_2), 50.17 ($C(CH_3)_3$)] were purchased from Millipore-Sigma and used as received. Diethyl ether, toluene, hexanes, and pentane were ACS Reagent grade, purified by an MBraun Solvent Purifier System, and stored over 4 Å molecular sieves for more than a day before use. Distilled water was degassed by sparging for 20 min. $PbCl_2$ was prepared by the addition of HCl (aq) (ca. 6 N) to an ice-cooled solution of $Pb(CH_3CO_2)_2$ (aq) (Baker, 95%) until precipitation ceased. The white precipitate was collected by filtration, dried under vacuum with heating (130 °C/10 mTorr), and stored in a dry box.

N, N'-di-*tert*-butylethylene-1,2-diimine (DAD)

N, N'-di-*tert*-butylethylene-1,2-diimine was prepared according to a modified literature procedure.[14] 2.4 eq. of neat *tert*-butylamine (150 mL, 1.44 mol) was added dropwise to a stirred 40 wt.% aqueous glyoxal (69 mL, 0.60 mol) in a round bottom flask on an ice bath under air. Shortly after addition is begun, DAD precipitates as a fluffy white crystalline solid. The heterogeneous suspension seized and resisted magnetic stirring as the full amount of *tert*-butylamine was added, so it was left overnight for the reaction to proceed completely. The next day the reaction has yielded a yellow-brown clear aqueous phase and a white precipitate. The precipitate is filtered under suction and washed with distilled water to yield an off-white crystalline powder. This solid was dissolved in a minimum of anhydrous Et_2O, dried over anhydrous $MgSO_4$, filtered through a medium porosity glass frit, and recrystallized at -20 °C to yield colourless prisms of *N*, *N′*-di-*tert*-butylethylene-1,2-diimine (65 g, 64.5% based on starting glyoxal). $\delta_{^1\mathrm{H}}$ NMR (300 MHz, C_6D_6, $\delta_{\mathrm{C_6}H_6} = 7.16$ ppm): 1.12 (18H, *s*, C(C*H*$_3$)$_3$), 8.07 (2H, *q*, N=C*H*)). $\delta_{^{13}\mathrm{C}}$ NMR (300 MHz, C_6D_6, $\delta_{C_6\mathrm{H}_6} = 128.39$ ppm): 29.71 (*s*, C(*C*H$_3$)$_3$), 58.20 (*s*, *C*(CH$_3$)$_3$), 157.92 (*s*, N=*C*H).

N, *N′*-di-*tert*-butylbutane-2,3-diamine

A dried 250 mL Schlenk flask was charged with 2.1 eq MeLi (100 mL, 1.6 M, 160 mmol) in a N_2-filled dry-box. In another flask, *N*, *N′*-di-*tert*-butylethylene-1,2-diimine (12.832 g, 76.3 mmol) was dissolved in about 50 mL of Et_2O, transfered to an addition funnel, and added with stirring to the MeLi at room temperature slowly enough to prevent boiling (ca. 2 h). After stirring for 3 h, the addition funnel was removed, the flask was closed with a rubber septum and removed from the dry-box, the solution cooled on an ice bath, and an excess of degassed H_2O (10 mL) was added. After stirring for an additional 30 minutes, the ethereal layer was isolated with a separation funnel, washed with brine, and dried over anhydrous $MgSO_4$. After removal of solvent at atmospheric pressure on a rotary-evaporator (10 °C condenser, 60 °C bath), the remaining oil is purified by distillation (b.p. ca. 90 celsius/1 Torr) to afford 13.464 g (88% based on starting diimine) of free diamine as a colourless oil. ^{1}H NMR spectra agreed with literature values.[14,33] $\delta_{^1\mathrm{H}}$ NMR (300 MHz, $CDCl_3$, $\delta_{\mathrm{Si}(CH_3)_4} = 0$ ppm): 0.96 (2H, *br*, N*H*), 1.04 (6H, *d*, C(H)C*H*$_3$), 1.08 (18H, *s*, C(C*H*$_3$)$_3$), 2.40 (2H, *q*, C(*H*)CH$_3$).

Bis[bis(trimethylsilyl)amido] lead(II) {Pb[N(SiMe$_3$)$_2$]$_2$}

Lithium bis(trimethylsilyl)amide (LiN(SiMe$_3$)$_2$) was prepared according to a previously detailed method from ^{n}BuLi (100 mL, 11.0 M in hexanes, 1.1 mol) and hexamethyldisilazane (195 g, 1.2 mol) in ca. 1 L of hexanes at room temperature to afford 169.2 g after distillation at 70 °C/10 mTorr (92%, based on ^{n}BuLi).[34] Pb[N(SiMe$_3$)$_2$]$_2$ was prepared according to a modified literature procedure.[35] Typically, in a N_2 filled dry-box, a 500 mL round-bottom flask was charged with 1.1 eq. $PbCl_2$

(14.49 g, 52 mmol) and 2 eq. $LiN(SiMe_3)_2$ (22.89 g, 95 mmol), 200 mL hexanes was added all at once, the flask was sealed with a greased glass stopper, and clipped shut to prevent escape of solvent during the exothermic salt-metathesis. The rate of reaction was conveniently limited by the relative insolubility of $PbCl_2$ in hydrocarbon solvents (note: use of diethyl ether consistently decreased final yield). Stirring was started and the reaction left overnight to complete. The next day, the flask contained a canary-yellow coloured supernatant with an off-white precipitate. Precipitated LiCl and excess $PbCl_2$ were removed by filtration over Celite, and solvent and free $HN(SiMe_3)_2$ were removed under reduced pressure at ambient temperature to afford $Pb[N(SiMe_3)_2]_2$ contaminated with $HN(SiMe_3)_2$ and $LiN(SiMe_3)_2$ as an orange-red oil. The impure product is not stable at room-temperature in the dark under inert atmosphere and purification by distillation is required. Vacuum distillation (90 °C/10 mTorr) over a small amount of $PbCl_2$ to consume remaining $LiN(SiMe_3)_2$ yields $Pb[N(SiMe_3)_2]_2$ (23.8 g, 95% based on $LiN(SiMe_3)_2$) as a thermochromic low-melting point solid that is ruby-red at 90 °C, orange at room temperature, yellow at −78 °C, and colourless at −196 °C. $\delta_{^1\mathrm{H}}$ NMR (300 MHz, C_6D_6, $\delta_{\mathrm{Si}(\mathrm{C}H_3)_4} = 0$ ppm): 0.96 (36H, *s*, Si(C*H*3)3). This procedure works equally well for the lighter congener $Sn[N(SiMe_3)_2]_2$.

Attempted synthesis of *rac-N*,^{2} *N* ^{3}-di-*tert*-butylbutane-2,3-diamido lead(II) (1Pb) via salt metathesis of $PbCl_2$

The dilithio diamidobutane salt was prepared as for the free diamine from DAD (3 g, 17.8 mmol) and MeLi (36.6 mmol), but was used in-situ rather than protonated as reported for **1Ge** and **1Sn**.[14] It was added with a dropping funnel over 2.5h to a stirred slurry of $PbCl_2$ in Et_2O cooled to −78 °C. A red soltuion and a black precipitate forms immediately. After addition, the slurry was stirred overnight. Cooling was not sustained and the solution warmed slowly to room-temperature. A red supernatant with black crystalline precipitate remained. All volatiles were removed under vacuum, leaving a grey residue. A small amount of a red oil, determined to be highly impure **1Pb** (ca. 5%, based on $PbCl_2$) by NMR, was vacuum distilled (70 °C/10 mTorr) from the residue. ^{1}H NMR on a benzene-d^6 extract of the residue revealed, among starting materials, peaks corresponding to acetaldehyde *tert*-butylimine $\delta(^1H)$ = 7.62 (q, 1H, CH=N) and δ = 1.71 (d, 3H, =C(H)CH_3).[32]

Successful preparation of 1Pb via transamination of $Pb[N(SiMe_3)_2]_2$

In a N_2 filled glove box, 1 eq. $L(NH)_2$ (0.92 g, 4.6 mmol) is added to 1 eq. $Pb[N(SiMe_3)_2]_2$ (2.41 g, 4.6 mmol) in 75 mL hexanes or toluene in an O-ring sealed, PTFE-capped, heavy-walled 150 mL pressure vessel. The mixture is heated to 70 °C for 3 days to completely convert $Pb[N(SiMe_3)_2]_2$ to **1Pb** as indicated by ^{1}H NMR. Less time will lead to incomplete conversion, higher temperatures lead to a decrease in yield due to decomposition, and we were unable to effectively separate $Pb[N(SiMe_3)_2]_2$ from **1Pb** by recrystallization or distillation. Slight decomposition is signaled by the precipitation of a black crystalline material—presumably Pb(0). The dark-red suspension is cooled to room-temperature and brought into a dry-box where it is filtered over Celite to remove the black precipitate, yielding a blood-red solution. Free $HN(SiMe_3)_2$ and solvent are removed under vacuum, and the impure residue is purified by vacuum-distillation (60 °C/10 mTorr) to afford **1Pb** (1.66 g, 89% based on $Pb[N(SiMe_3)_2]_2$) as an extremely air- and moisture-sensitive blood-red crystalline solid. Samples slowly darken upon standing in light under inert atmosphere after > 2 weeks. M.p. 53 °C, distilled. Found: C, 35.0; H, 6.3; N, 7.1. $C_{12}H_{26}N_2Pb$ requires: C, 35.5; H, 6.5; N, 6.9%. HRMS (EI) Found, m/z = 406.18570, calc. 406.1864, dev. −0.54‰. $\delta_{^1\mathrm{H}}$ NMR (300 MHz, C_6D_6, $\delta_{C_6H_6}$ = 7.16 ppm): 1.35 (18H, *s*, C(CH_3)$_3$), 1.45 (6H, *d*, C(H)CH_3), 5.37 (2H, *q*, C(H)CH$_3$)). $\delta_{^{13}\mathrm{C}}$ NMR (300 MHz, C_6D_6, $\delta_{C_6H_6}$ = 128.06 ppm): 30.53 (C(H)CH$_3$), 35.07 (C(CH$_3$)$_3$), 59.42 (C(CH$_3$)$_3$), 73.61 (C(H)CH$_3$).

Characterization

In-situ NMR of the attempted preparation of 2Pb

In a drybox, $Pb[N(SiMe_3)_2]_2$ (0.143 g, 0.27 mmol) was dissolved in dry, degassed C_6D_6 (ca. 1 mL) in an NMR tube, closed with a plastic cap, and sealed with Parafilm. *N*, *N′*-di-*tert*-butylethylene-1,2-diamine (0.048 g, 0.28 mmol) was also dissolved in C_6D_6 (ca. 0.5 mL) in a small vial and capped with a rubber septum. A spectrum was obtained of $Pb[N(SiMe_3)_2]_2$, then the tube was removed from the spectrometer and the diamine solution was injected with a syringe through the cap all at once. The NMR tube was resealed with more Parafilm, shaken vigorously for approximately 30 s, and placed back in the spectrometer. The sample was locked and shimmed before each acquisition, when 16 scans were acquired.

Thermogravimetric analysis (TGA)

TGA was performed with a TA Instruments Q50 kept in an MBraun Labmaster 130 dry-box filled with N_2. Pt pans were coated before each experiment with approximately 55 nm of Al_2O_3 by atomic layer deposition (ALD) in a Picosun R-100 reactor using 500 cycles of trimethylaluminum (TMA) and water at 200 °C with 0.1 s pulses and 8 s purges each. This is critical to protect the Pt pans as they become brittle and break easily after high-temperature exposure to Pb(0) residues from precursor decomposition. The TGA furnace was purged with 99.999% N_2 at 60 sccm temperature was increased at 10 °C min^{-1} for the "ramp" experiments, and increased at 40 °C min^{-1} to increase temperatures step-wise to hold at isotherms of 60–130 °C for 7 min each for the "stepped isothermal" experiments. The exact masses for the 10 mg, 20 mg, and 40 mg loadings shown in Figure 4 were 11.61886 mg, 20.40275 mg, and 39.35869 mg, respectively.

In-situ NMR thermolysis of 1Pb

^{1}H and ^{13}C NMR spectra were obtained after heating a 15 mM solution of **1Pb** in toluene-d^8 in a sealed heavy-walled glass tube at 90 °C for 7 days. Spectra were collected, every 12 h after cooling the sample to room-temperature. At 90 °C, formation of a black precipitate and signals corresponding to the free ligand $L(NH)_2$ (see above) appeared. This same sample was subjected to 6 h at 150 °C as before, and spectra were obtained after cooling. Low-resolution spectra were obtained due to poor shimming from suspended particles, but a signal at high chemical shift ($\delta \sim 7.6$ ppm) was observed by ^{1}H NMR that prompted another decomposition study.

Neat thermolysis of 1Pb

1Pb (0.302 g, 0.74 mmol) was placed in a 50 mL Schlenk flask in a dry-box and placed under a strong over-pressure of ultra-pure Ar (99.999%) on a Schlenk line. It was then joined to a previously flame-dried reflux condenser fitted with a gas inlet at the top, and heated to 150 °C with an oil bath for 6 h. After cooling, the black residue was extracted with anhydrous (stored over 4 Å sieves), degassed benzene-d^6 and transfered to a dried NMR tube under a stream of ultra-pure N_2 (99.999%). The dark-brown, murky sample was analyzed immediately by ^{1}H and COSY NMR, and a ^{13}C NMR spectrum (14 336 scans) was obtained overnight. Another ^{1}H spectrum was obtained the following day, which showed essentially the same spectrum with better resolution since the suspended Pb(0) solids had settled. Clear signals corresponding to an imino hydrogen [$\delta(^1H)$ = 7.62 (q, 1H, CH=N)] that correlated (COSY) to another signal [δ = 1.71 (d, 3H, =C(H)CH_3)] presumably belonging to acetal hydrogens. The *tert*-butyl region was obscured by signals from free diamine ligand and surviving **1Pb**; the origin of the protonated diamine remains unclear. The emergent signals correpsond to the reported chemical shifts of acetaldehyde *tert*-butylimine.[32] We were unable to determine which enantiomer was formed in the scope of this study.

Single-crystal X-ray diffraction of 1Pb

1Pb is highly soluble in polar non-protic and antipolar non-protic solvents such as diethyl ether, tetrahydrofuran, n-hexane, n-pentane and toluene. Crystals suitable for single-crystal X-ray diffraction (scXRD) were grown by recrystallization of distilled **1Pb** in a 1:1 mixture of diethyl ether and toluene at -30 °C, coated with Paratone-N oil, mounted on a fiber loop, and placed in a cold, gaseous N_2 stream on a Rigaku-Oxford SuperNova diffractometer performing ϕ and ω scans at 100 K. Diffraction intensities were measured using graphite monochromatic Cu Kα radiation (λ = 1.54184 Å). Data collection, indexing, initial cell refinements, frame integration, final cell refinements, and absorption corrections were accomplished with Agilent CrysAlis Pro v1.171.37.34. Space groups were assigned by analysis of the metric symmetry and systematic absences (determined by WinGX) and were further checked by PLATON[36] for additional symmetry. The structure was solved with ShelxT and refined against all data in the reported 2θ ranges by full-matrix least-squares on F^2 with the SHELXL program suite using the ShelxLe interface.[37] Stucture images were rendered with ORTEP3.[38] The data was deposited in the Cambridge Structural Database (CSD) with indentification number: CCDC 1587313.

Powder X-ray diffraction

Bulk purity was assessed by powder X-ray diffraction (pXRD), see Supplementary Information. A theoretical diffraction pattern of **1Pb** was calculated based on the structural data set obtained by scXRD (see above) by Crystal Impact DIAMOND v3.2. The simulation was carried out for the 2θ angle range of 5° to 60° from irradiation of a Cu Kα X-Ray source. 50 mg of **1Pb** were ground in a pestle-and-mortar in a dry-box, then carefully filled in a glass capillary (Mark capillary for X-Ray microstructure analysis). The capillary was sealed with grease, flame sealed, mounted on a rotatable sample holder and geometrically aligned to avoid static imbalance during the measurement. The pXRD experiments was conducted with a Bruker D8 Advance diffractometer [X-Ray source Cu Kα (λ = 1.54184 Å), 40 kV, 30 mA] in Bragg-Brentano geometry in a 2θ range of 5° to 60°. Diffraction data were processed using Bruker AXS Diffrac$^{\text{plus}}$ EVA v10.0.

References

(1) Hoffmann-Eifert, S.; Watanabe, T. In *Atomic Layer Deposition for Semiconductors*; Hwang, C. S., Ed.; Springer US: Boston, MA, 2014; pp 149–171, DOI: 10.1007/978-1-4614-8054-9_6.

(2) Ono, L. K.; Juarez-Perez, E. J.; Qi, Y. Progress on Perovskite Materials and Solar Cells with Mixed Cations and Halide Anions. *ACS Appl. Mater. Interfaces* **2017**, *9*, 30197–30246.

(3) others,, et al. Revisiting the valence and conduction band size dependence of PbS quantum dot thin films. *ACS nano* **2016**, *10*, 3302–3311.

(4) Dasgupta, N. P.; Lee, W.; Prinz, F. B. Atomic layer deposition of lead sulfide thin films for quantum confinement. *Chem. Mater.* **2009**, *21*, 3973–3978.

(5) Ellingson, R. J.; Beard, M. C.; Johnson, J. C.; Yu, P.; Micic, O. I.; Nozik, A. J.; Shabaev, A.; Efros, A. L. Highly efficient multiple exciton generation in colloidal PbSe and PbS quantum dots. *Nano Lett.* **2005**, *5*, 865–871.

(6) Sukhovatkin, V.; Hinds, S.; Brzozowski, L.; Sargent, E. H. Colloidal quantum-dot photodetectors exploiting multiexciton generation. *Science* **2009**, *324*, 1542–1544.

(7) Krisyuk, V. V.; Turgambaeva, A. E.; Igumenov, I. K. Volatile Lead β-Diketonates as CVD Precursors. *Chem. Vap. Deposition* **1998**, *4*, 43–46.

(8) Ramesh, R.; Aggarwal, S.; Auciello, O. Science and technology of ferroelectric films and heterostructures for non-volatile ferroelectric memories. *Mater. Sci. Eng., R* **2001**, *32*, 191–236.

(9) Miikkulainen, V.; Leskelä, M.; Ritala, M.; Puurunen, R. L. Crystallinity of inorganic films grown by atomic layer deposition: Overview and general trends. *J. Appl. Phys.* **2013**, *113*, 2.

(10) Asay, M.; Jones, C.; Driess, M. N-Heterocyclic carbene analogues with low-valent group 13 and group 14 elements: syntheses, structures, and reactivities of a new generation of multitalented ligands. *Chem. Rev* **2011**, *111*, 354–396.

(11) Blom, B.; Gallego, D.; Driess, M. N-heterocyclic silylene complexes in catalysis: new frontiers in an emerging field. *Inorg. Chem. Front.* **2014**, *1*, 134–148.

(12) Benedek, Z.; Szilvási, T. Theoretical Assessment of Low-Valent Germanium Compounds as Transition Metal Ligands: Can They Be Better than Phosphines or NHCs? *Organometallics* **2017**, *36*, 1591–1600.

(13) Vepřek, S.; Prokop, J.; Glatz, F.; Merica, R.; Klingan, F.; Herrmann, W. Organometallic

chemical vapor deposition of germanium from a cyclic germylene, 1, 3-Di-tert-butyl-1, 3, 2-diazagermolidin-2-ylidine. *Chem. Mater.* **1996**, *8*, 825–831.

(14) Kim, S. B.; Sinsermsuksakul, P.; Pike, R. D.; Gordon, R. G. Synthesis of N-Heterocyclic Stannylene (Sn (II)) and Germylene (Ge (II)) and a Sn (II) Amidinate and Their Application as Precursors for Atomic Layer Deposition. *Chem. Mater.* **2014**, *26*, 3065–3073.

(15) Gans-Eichler, T.; Gudat, D.; Nieger, M. Tin Analogues of Arduengo Carbenes: Synthesis of 1, 3, 2λ2-Diazastannoles and Transfer of Sn Atoms between a 1, 3, 2λ2-Diazastannole and a Diazadiene. *Angew. Chem., Int. Ed.* **2002**, *41*, 1888–1891.

(16) Charmant, J. P.; Haddow, M. F.; Hahn, F. E.; Heitmann, D.; Fröhlich, R.; Mansell, S. M.; Russell, C. A.; Wass, D. F. Syntheses and molecular structures of some saturated N-heterocyclic plumbylenes. *Dalton Trans.* **2008**, 6055–6059.

(17) Artus, G. CCDC 123898. *CSD Communication* **1996**, DOI: `10.5517/cc44xqw`.

(18) Hahn, F. E.; Heitmann, D.; Pape, T. Synthesis and Characterization of Stable N-Heterocyclic Plumbylenes. *Eur. J. Inorg. Chem.* **2008**, *2008*, 1039–1041.

(19) Coyle, J. P.; Gordon, P. G.; Wells, A. P.; Mandia, D. J.; Sirianni, E. R.; Yap, G. P.; Barry, S. T. Thermally robust gold and silver iminopyrrolidinates for chemical vapor deposition of metal films. *Chem. Mater.* **2013**, *25*, 4566–4573.

(20) Li, W.; Hill, N. J.; Tomasik, A. C.; Bikzhanova, G.; West, R. A new monomeric saturated N-heterocyclic silylene as a racemic mixture. *Organometallics* **2006**, *25*, 3802–3805.

(21) Haaf, M.; Schmedake, T. A.; West, R. Stable silylenes. *Acc. Chem. Res.* **2000**, *33*, 704–714.

(22) Arduengo III, A. J.; Bock, H.; Chen, H.; Denk, M.; Dixon, D. A.; Green, J. C.; Herrmann, W. A.; Jones, N. L.; Wagner, M.; West, R. Photoelectron spectroscopy of a carbene/silylene/germylene series. *J. Am. Chem. Soc.* **1994**, *116*, 6641–6649.

(23) Blom, B.; Said, A.; Szilvási, T.; Menezes, P. W.; Tan, G.; Baumgartner, J.; Driess, M. Alkaline-Earth-Metal-Induced Liberation of Rare Allotropes of Elemental Silicon and Germanium from N-Heterocyclic Metallylenes. *Inorg. Chem.* **2015**, *54*, 8840–8848.

(24) Herrmann, W. A.; Denk, M.; Behm, J.; Scherer, W.; Klingan, F.-R.; Bock, H.; Solouki, B.; Wagner, M. Stable cyclic germanediyls (cyclogermylenes): Synthesis, structure, metal complexes, and thermolyses. *Angew. Chem., Int. Ed.* **1992**, *31*, 1485–1488.

(25) Coyle, J. P.; Sirianni, E. R.; Korobkov, I.; Yap, G. P.; Dey, G.; Barry, S. T. Study of Monomeric Copper Complexes Supported by N-Heterocyclic and Acyclic Diamino Carbenes. *Organometallics* **2017**, *36*, 2800–2810.

(26) Fjeldberg, T.; Hope, H.; Lappert, M. F.; Power, P. P.; Thorne, A. J. Molecular structures of the main group 4 metal (II) bis (trimethylsilyl)-amides M [N (SiMe 3) 2] 2 in the crystal (X-ray) and vapour (gas-phase electron diffraction). *J. Chem. Soc., Chem. Commun.* **1983**, 639–641.

(27) Heitmann, D.; Pape, T.; Hepp, A.; Muck-Lichtenfeld, C.; Grimme, S.; Hahn, F. E. Palladium and platinum complexes of a benzannulated n-heterocyclic plumbylene with an unusual bonding mode. *J. Am. Chem. Soc.* **2011**, *133*, 11118–11120.

(28) Horchler, K.; Stader, C.; Wrackmeyer, B. Monomeric 1, 4, 2, 3, 5λ2-diazadisilastannolidines and-plumbolidines. *Inorg. Chim. Acta* **1986**, *117*, L39–L40.

(29) Wrackmeyer, B.; Stader, C.; Horchler, K.; Zhou, H.; Schlosser, D. Dimeric cyclic bis (amino) stannylenes and-plumbylenes-a multinuclear magnetic resonance study. *Inorg. Chim. Acta* **1990**, *176*, 205–214.

(30) Coyle, J. P.; Kurek, A.; Pallister, P. J.; Sirianni, E. R.; Yap, G. P.; Barry, S. T. Preventing thermolysis: precursor design for volatile copper compounds. *Chem. Commun.* **2012**, *48*, 10440–10442.

(31) Kunte, G.; Shivashankar, S.; Umarji, A. Thermogravimetric evaluation of the suitability of precursors for MOCVD. *Meas. Sci. Technol.* **2008**, *19*, 025704.

(32) Mann, S.; Carillon, S.; Breyne, O.; Marquet, A. Total synthesis of amiclenomycin, an inhibitor of biotin biosynthesis. *Chem. Eur. J.* **2002**, *8*, 439–450.

(33) Gardiner, M. G.; Raston, C. L. Carbolithiations of N, N'-Di-tert-butyl-1, 4-diazabuta-1, 3-diene. *Inorganic Chemistry* **1995**, *34*, 4206–4212.

(34) Amonoo-Neizer, E.; Shaw, R.; Skovlin, D.; Smith, B.; Rosenthal, J. W.; Jolly, W. L. Lithium bis (trimethylsilyl) amide and tris (trimethylsilyl) amine. *Inorg. Synth.* **1966**, *8*, 19–22.

(35) Harris, D. H.; Lappert, M. F. Monomeric, volatile bivalent amides of group IV B elements, M (NR 1 2) 2 and M (NR 1 R 2) 2 (M [double bond, length half m-dash] Ge, Sn, or Pb; R 1 [double bond, length half m-dash] Me 3 Si, R 2 [double bond, length half m-dash] Me 3 C). *J. Chem. Soc., Chem. Commun.* **1974**, 895–896.

(36) Spek, A. L. Structure validation in chemical crystallography. *Acta Crystallographica Section D: Biological Crystallography* **2009**, *65*, 148–155.

(37) Sheldrick, G. M. Crystal structure refinement with SHELXL. *Acta Crystallographica Section C: Structural Chemistry* **2015**, *71*, 3–8.

(38) Farrugia, L. J. WinGX and ORTEP for Windows: an update. *Journal of Applied Crystallography* **2012**, *45*, 849–854.